Liquefaction susceptibility for the region of Evansville, IN

USGS Final Technical Report #07HQGR0058

Date 5/23/2008
Version 9

Yoon Seok Choi[1]
Jennifer S. Haase[2]
Robert L. Nowack[2]

Department of Civil Engineering
Purdue University
West Lafayette, IN 47906

Department of Earth and Atmospheric Sciences
Purdue University
West Lafayette, IN 47906

Corresponding author:
Jennifer Haase
765-594-8677
765-496-1210 (fax)
jhaase@purdue.edu

Abstract

Evansville, Indiana, located on the banks of the Ohio River, is susceptible to liquefaction-induced damage in the event of significant earthquake shaking. The city is currently the subject of an urban seismic hazard investigation because of its proximity to the New Madrid seismic zone, where a sequence of three earthquakes with magnitude greater than 7 occurred in 1811-1812, as well as the Wabash fault zone which produced a major earthquake approximately 4000 years ago. This study calculates liquefaction susceptibility maps for the Evansville area, as a complement to recent work on the probabilistic seismic hazard analysis (Haase et al., 2006). The peak ground acceleration with 2% probability of being exceeded in 50 years is 0.3 g for much of the study region and as much as 0.4-0.5 g at the river basin edges. These acceleration levels are important to consider in the study of liquefaction for the Evansville area.

Recently acquired cone penetrometer test data are used to estimate the factor of safety against liquefaction at 58 sites in the study region. The unconsolidated sediments within the study region are grouped into 3 subregions based on common material properties. The liquefaction potential index (LPI) is calculated to map the spatial variability of liquefaction susceptibility. Since there are high uncertainties in the characterization of the soil column due to horizontal spatial variability, a probabilistic method is adopted for the susceptibility mapping. It is based on the statistical characteristics of the material properties within each subregion. The resulting maps for scenario earthquakes of magnitude 6.5 and 7.7 show the mean LPI, and the probability that the LPI is greater than threshold values of 5 and 15. The LPI is high in the river alluvium subregion, where the soil profiles contain predominantly sand. The maps also show a contrasting region of lacustrine deposits that predominantly include clayey soil with a lower liquefaction susceptibility. The soil profiles within the deposits of terrace alluvium deposits are more complex as they contain highly variable sequences of silty sand, clayey sand, and sandy clay. Since there is less consistency of the liquefaction potential index within this subregion, a probabilistic approach is more appropriate for liquefaction susceptibility mapping.

1 Introduction

Evansville, Indiana, is a current target for urban seismic hazard mapping in the Central US because of its proximity to the New Madrid seismic zone, where a sequence of three Earthquakes with magnitude greater than 7 occurred in 1811-1812 (Hough et al., 2000). Both the New Madrid and the Wabash Valley fault zones are potential source areas for triggering liquefaction in and around Evansville, which lies on sequences of alluvial and lacustrine sediments adjacent to the Ohio River. Nearby quarries and streambeds show evidence of historic liquefaction, due to an event in the Wabash fault zone or south central Indiana approximately 4000 years ago (Munson et al., 1995; Obermeier, 1996).

This study constructs liquefaction susceptibility maps for the Evansville area, as a complement to recent work on the probabilistic seismic hazard for the region (Haase et al., 2006). The probabilistic seismic hazard assessment was carried out using subsurface information on shear wave velocity and depth to bedrock to incorporate probabilistically the near-surface amplification due to local site effects. That study revealed that the surficial geologic units present in the river alluvium in the low-lying regions and in the loess covered uplands had significantly different properties that affected the spatial distribution of amplification and thus the expected acceleration levels. Within the deepest sediments of the Ohio River valley, distinct resonant natural periods between 0.6 to 0.8 s created high amplification at 1 s period. There was also some amplification at higher frequencies outside the river basin. However, because of nonlinearity in the response of the soil profiles, there was significant de-amplification that reduced expected acceleration levels for much of the area. The peak ground acceleration (PGA) with 2% probability of being exceeded is 0.3 g for much of the study region, with values at the river basin edges as high as 0.4-0.5 g. These variations in acceleration levels are important to consider in a study of liquefaction. The probabilistic seismic hazard maps were de-aggregated (Harmsen et al., 1999) to investigate what earthquake magnitude and distance contributed to the seismic hazard for the Evansville region. It was found that a magnitude 5.9 to 6.5 earthquake contributed significantly to the hazard for peak ground acceleration, and a magnitude 7.7 earthquake at 170 km distance (i.e. a New Madrid-type event) contributed significantly to the seismic hazard for spectral accelerations at 1 Hz for 2% probability of exceedence in 50 years.

Several recent studies have investigated the soil conditions present along the Wabash and Ohio rivers and evaluated the seismic hazard from liquefaction. Ground accelerations and liquefaction potential were evaluated for 9 sites in southwestern Indiana in order to estimate the damage potential to pile foundations at bridge sites (Bobet et al., 2001). Soil liquefaction and lateral spreading were found to be likely to occur in the deep alluvial deposits of both the Ohio and Wabash river valleys. A study of the glacial outwash deposits at the boundary of the river alluvium in Evansville was carried out using a combination of standard penetration test (SPT) data and cone penetrometer test (CPT) data and showed that the liquefaction hazard had a large range in these units (Kayabali, 1993). These studies investigated individual sites but did not provide an estimate of liquefaction hazard over the entire Evansville region.

Several approaches have been developed to provide an integrated map view of liquefaction hazard, which otherwise depends on depth dependent soil characteristics. Holzer et al. (2006) used cumulative frequency distributions of the liquefaction potential index (LPI) of surficial geologic units to evaluate the liquefaction potential in the Greater Oakland, California, Area. They calculated LPI values for each CPT sounding based on M 6.6 and 7.1 scenario earthquakes and determined the percentage of area predicted to liquefy for each earthquake. Lenz and Baise (2007) evaluated the spatial variability of LPI in the same area using CPT and SPT data. They suggested that a geo-statistical method for the interpolation of LPI is appropriate to construct a detailed liquefaction map. A study based on the method of Holzer et al. (2006) was carried out in Shelby County (Memphis), Tennessee, to calculate a liquefaction susceptibility map (Rix and Romero-Hudock, 2003), and used a scenario earthquake on the New Madrid fault.

In the Evansville area, cone penetrometer test (CPT) data have been collected that sample the principal surficial geologic units (Holzer, 2003). These data and the other datasets used in this study are described in section 2. For the first part of this study, the factor of safety against liquefaction for each CPT location is calculated using the method of Robertson and Wride (1998) based on the cyclic resistance ratio and cyclic stress ratio and the properties of the soil column. The method is described in section 3 and the results are presented in section 4. In section 5 the statistics of the soil properties are investigated, and a probabilistic method is adopted for the second part for calculations of the Liquefaction Potential Index (LPI), which is then used to map the spatial variability of the liquefaction susceptibility. Section 6 gives a discussion comparing the results to previous work and addresses inconsistencies with SPT measurements. The conclusions are summarized in section 7.

2 Data

As part of a study of the probabilistic hazard of ground shaking in the Evansville region (Haase et al., 2006) surficial geologic mapping was carried out at 1:24000 scale for 7 of the 9 USGS map quadrangles surrounding the city of Evansville in the southwestern part of Indiana (Moore et al., 2007). The region was mapped using 11 units based on lithology and depositional environment. For the Daylight and Kasson quads (northwestern and northeastern quads), the previously available surficial geologic maps at 1:500,000 scale (Gray, 1989) were used, with revisions to the nomenclature for the units to be consistent with the recent mapping.

The surficial geology along the Ohio River valley near Evansville consists of a variety of glacial and interglacial lithologic sequences characterized by a series of fluvial and lake depositional events, and later deposition of relatively thick Ohio River fluvial deposits (Eggert et al., 1996; Eggert et al., 1997a; Eggert et al., 1997b) (Figure 1). These deposits include alluvium and outwash (Qal) and are composed of chiefly fine- to medium-grained, lithic quartz sand, interbedded with lenses of clay, clayey silt, silt, coarse sand, granules, and gravel (Moore et al., 2007). The typical depositional sequence consists of gravelly

sand to sandy gravel at greater depth, predominantly sand in the middle, and silt and clay at the top. Ancient valleys of tributaries to the Ohio River are filled with silty and clayey lacustrine terrace deposits (Qlt). The surficial geology in the northern portions of the Evansville region includes loess (Ql) covering the bedrock and lacustrine units.

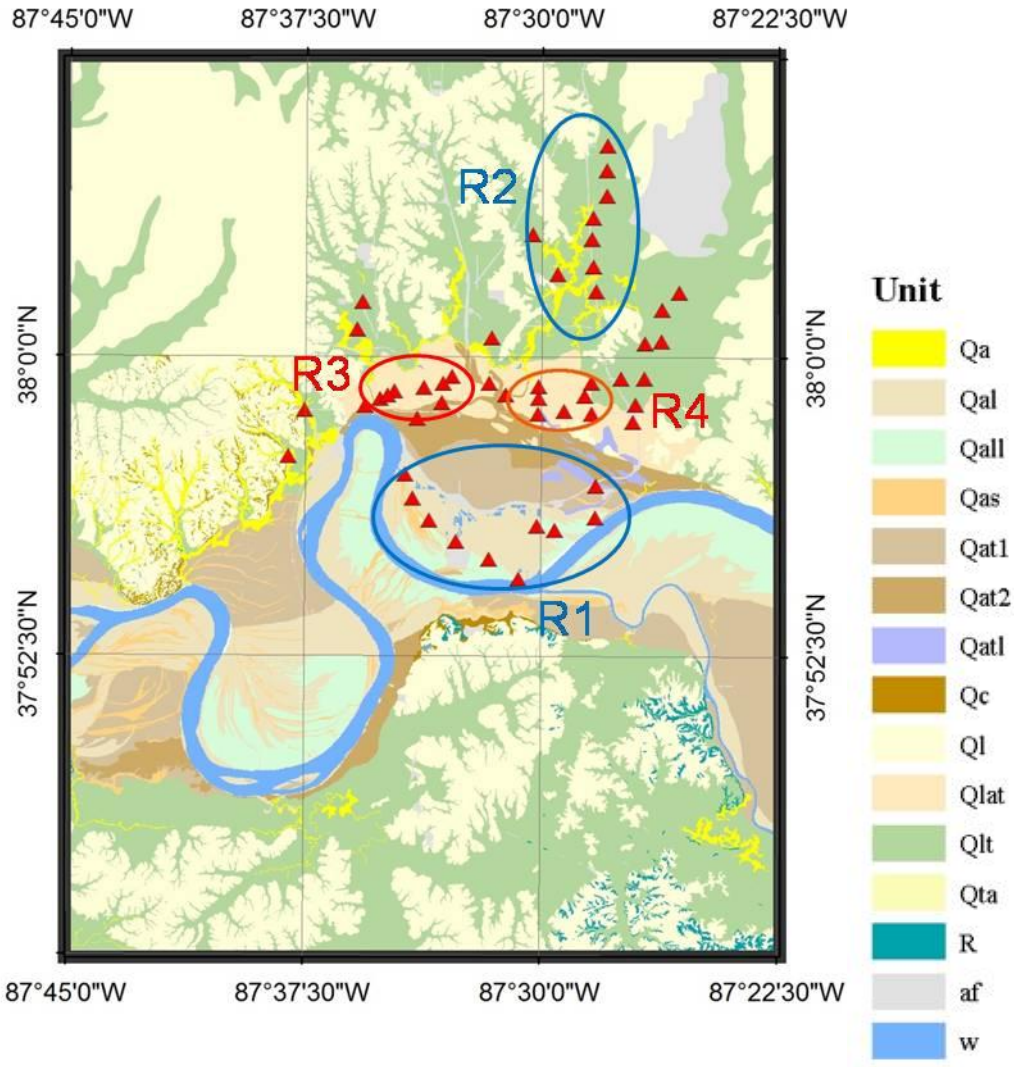

Figure 1 Surficial geologic map (Moore et al., 2007). Qa: Creek alluvium and sheetwash alluvium, Qal: River floodplain alluvium, Qall: River alluvium, Qas: Alluvium in sloughs, Qat1: River terrace alluvium, Qat2: River terrace alluvium, Qatl: Paleolevees on terrace alluvium, Qc: Colluvium, Ql: Loess, Qlat: Terrace alluvium and paleolevee deposit, Qlt: Lacustrine terrace deposit, Qta: Creek alluvium, af: Artificial fill, R: Bedrock, w: surface water (Ohio river). Also shown are the locations of the CPT profiles and subgroup for analysis, R1: Subgroup-1 river alluvium profiles, R2: Subgroup-2 lacustrine profiles, R3: Subgroup-3 western terrace alluvium profiles, and R4: Subgroup-3 eastern terrace alluvium profiles.

Liquefaction assessment is dependent on the ground water table since liquefaction requires saturated soil, and since the effective stresses of the soil that determine the resistance to liquefaction depend on the depth below the water table. The ground water table information is collected from water well logs from the Indiana Geological Survey (IGS) and the Kentucky Geological Survey (KGS) (Figure 2). Development of detailed contours based on all available data is required. The nine hundred water well logs and individual water well depth points contain information on surface elevation, static water table and depth to bedrock, so the depth to ground water table can be obtained directly from these data. The smoothed and interpolated ground water table surface was generated using local polynomial interpolation. The uncertainty in this estimate of the groundwater table is 7.2 m, based on the differences between the point data and the interpolated surface, however seasonal and interannual variations in groundwater were not investigated and may be larger. The ground water table is higher within the regions near the river, which are categorized as alluvium on the surficial geologic map. Therefore, the liquefaction susceptibility in this region will be greater than in the other areas due to the presence of sandy soil within the region of higher ground water table elevation. The uncertainty in the ground water table depth influences the liquefaction hazard at a given site, and this variability is considered when calculating the distribution of LPI.

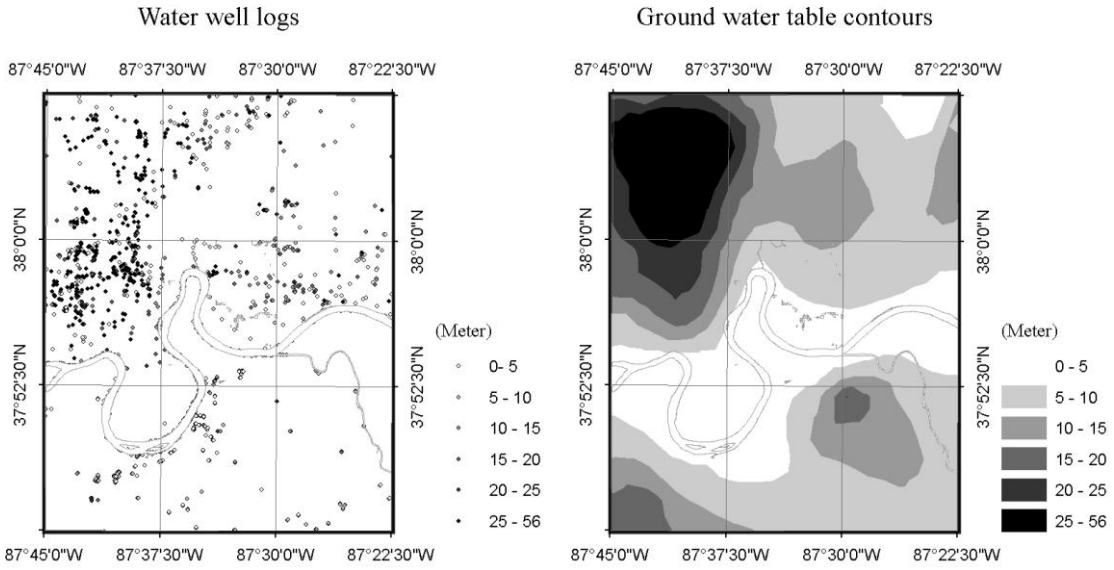

Figure 2 a) Water well logs used for the interpolation of the ground water table. b) smoothed and interpolated ground water table contours in meters below the surface.

Cone penetrometer tests were carried out at 58 sites (Holzer, 2003). Tip resistance, sleeve friction, and shear wave travel time were measured at each site. Soil type was determined indirectly using the method of Robertson and Wride (1998). Among these, ten CPT measurements were carried out in the alluvial unit, twenty CPT measurements in lacustrine units, and eighteen CPT measurements in the alluvial terrace unit (Figure 1).

An example of the CPT data from one site is shown in Figure 3. Several profiles constituting cross-sections through the different units are provided in the appendix.

To evaluate the liquefaction susceptibility, the method of Youd et al. (2001) is used. Two values are required to calculate the factor of safety for liquefaction: the seismic demand on a soil layer, and the soil capacity to resist liquefaction. The factor of safety (FS) is calculated as a function of the cyclic resistance ratio (CRR) for a magnitude 7.5 earthquake, $CRR_{7.5}$, cyclic stress ratio, CSR, and a magnitude scaling factor, MSF, given by

$$FS = \left(\frac{CRR_{7.5}}{CSR} \right) \cdot MSF \qquad (1)$$

The MSF is given by Youd and Noble (1997) for different probabilities of liquefaction occurrence, P_L, , as specified below:

$$\text{Probability } 0 < P_L < 20\% \quad MSF = \frac{10^{3.81}}{M_w^{4.53}} \text{ for } M_w < 7$$

$$\text{Probability } 20\% < P_L < 32\% \quad MSF = \frac{10^{3.74}}{M_w^{4.33}} \text{ for } M_w < 7 \qquad (2)$$

$$\text{Probability } 32\% < P_L < 50\% \quad MSF = \frac{10^{4.21}}{M_w^{4.81}} \text{ for } M_w < 7.75$$

A lower bound for the MSF is defined by the following equation (Youd et al., 2001):

$$MSF = \frac{10^{2.24}}{M_w^{2.56}} \qquad (3)$$

The simplified equation for cyclic stress ratio (CSR) quantifies the stresses produced in the soil by an earthquake and is given by

$$CSR = 0.65 \left(\frac{a_{\max}}{g} \right) \left(\frac{\sigma_{v0}}{\sigma'_{v0}} \right) r_d \qquad (4)$$

where $a_{\max}$ is the peak ground surface acceleration, g is the acceleration of gravity, σ_{v0} is the total vertical stress and r_d is the stress reduction factor at the depth of interest. The average effective vertical stress, σ'_{v0} , is a function of depth below the water table. Using the simplified method of Youd et al. (2001), the stress reduction factor as a function of depth, *z*, is approximated by

$$r_d = \frac{1.000 - 0.4113 \cdot z^{0.5} + 0.04052 \cdot z + 0.001753 \cdot z^{1.5}}{1.000 - 4.177 \cdot z^{0.5} + 0.05729 \cdot z - 0.006205 \cdot z^{1.5} + 0.001210 \cdot z^{2}} \quad (5)$$

The liquefaction resistance of the soil is quantified with the cyclic resistance ratio, CRR obtained from field cone penetrometer test data (CPT) or standard penetration tests (SPT). For CPT data, the CRR is related to cone penetration tip resistance q_{c1N} corrected to a clean sand and normalized to 100 kPa and is given by

$$CRR_{7.5} = \begin{cases} 0.833\left[\dfrac{(q_{c1N})_{cs}}{1000}\right] + 0.05 & \text{if } (q_{c1N})_{cs} < 50 \\ 93\left[\dfrac{(q_{c1N})_{cs}}{1000}\right] + 0.08 & \text{if } 50 \le (q_{c1N})_{cs} < 160 \end{cases} \quad (6)$$

The normalized cone tip resistance, q_{c1N}, is corrected for overburden stress in the following manner

$$q_{c1N} = \left(\frac{q_c}{P_a}\right) C_Q \quad \text{with} \quad C_Q = \left(\frac{P_a}{\sigma'_{v0}}\right)^n \quad (7)$$

where P_a is the atmospheric pressure and equal to 100 kPa, C_Q is the normalizing factor for cone penetration resistance, n is an exponent that varies with soil type and q_c is the cone tip resistance measured in the field. A correction factor, K_c, which is a function of soil behavior type index, I_c, is applied to correct for the fines content in the soil as

$$(q_{c1N})_{cs} = K_c q_{c1N} \quad (8)$$

where

$$K_c = \begin{cases} 1.0 \text{ for } I_c \le 1.64 \\ -0.403 I_c^4 + 5.581 I_c^3 - 21.63 I_c^2 + 33.75 I_c - 17.88 \text{ for } I_c > 1.64 \end{cases} \quad (9)$$

The soil behavior type index, I_c, is a function of the cone tip resistance q_c and the measured sleeve resistance, f_s, and is given by

$$I_c = \left[(3.47 - \log Q)^2 + (1.22 + \log F)^2\right]^{0.5} \quad (10)$$

where

$$Q = \left[\frac{(q_c - \sigma_{v0})}{P_a}\right]\left[\frac{P_a}{\sigma'_{v0}}\right]^n \quad (11)$$

and

$$F = 100\left[\frac{f_s}{(q_c - \sigma_{vo})}\right] \qquad (12)$$

Here, n is 0 or 1 depending on the type of soil. An example showing the CPT measurements of tip resistance and sleeve friction for a typical profile located in the river alluvium is shown in Figure 3a and b. It has 6 m of clay overlying a 5 m sequence of silt and silty sand, overlying 9 meters of old Ohio river sands and gravels (Figure 3c), as identified in the soil behavior type index (Figure 3f). The sequence of calculations for the factor of safety is shown in Figure 3d through j. Figure 3d shows the tip resistance normalized by the overburden stress, which adjusts the measurements for the higher tip resistance found under higher confining stress at depth. The near surface (top 2 m) in the clay layer has a relatively high corrected tip resistance (Figure 3i) leading to a sufficiently high factor of safety to inhibit liquefaction. I_c and K_c are necessary to correct soils with fines content to a reference clean sand. In this example I_c and K_c are high in the top layer, which is identified as clay. The intermediate depth sequence also indicates significant fines content leading to a moderate correction factor K_c. The intermediate depth silty sand unit has a slow increase in CSR due to the increase in effective vertical stress below the water table (Figure 3j). In addition, this layer has a relatively low corrected tip resistance and a low sleeve friction. This leads to a low factor of safety. Figure 3k and Figure 3l shows that many points in the clay unit that have a low factor of safety are excluded from the calculation of liquefaction potential index because they have been identified as units with $I_c > 2.6$, that is, they are not susceptible to liquefaction because of their very high clay content. Overall, the liquefaction potential index is high for this site because of the low factor of safety in this intermediate depth silty sand sequence (Figure 3k).

The factor of safety is calculated for each soil element at a particular depth. The liquefaction potential index, LPI, integrates this information over the entire profile and gives a single number that is representative of the probability that any of the susceptible elements will liquefy. The LPI is defined by Iwasaki, et al. (1982),

$$LPI = \int_{0m}^{20m} F \cdot w(z)\, dz$$

$$where,\ F = \begin{cases} 1 - FS & for\ FS \le 1 \\ 0 & for\ FS > 1 \end{cases} \qquad (13)$$

$$w(z) = 10 - 0.5z$$

and z is the depth from the ground surface in meters. The weights in the integrand tend to reduce the overall influence of the contributions from deep soil layers. LPI can be considered as a function of the thickness of the liquefiable layer, the proximity of the liquefiable layer to the surface, and the value of the layer's factor of safety when the factor safety (F.S.) is less than 1. Note that most clay and silty clay layers are excluded from the calculation when their soil behavior index I_c is less than 2.6. So in the example above, most of the soil elements in the shallow and intermediate depths (clay and silty

clay) are excluded from the integral. This will be discussed in more detail in section 3.4. The liquefaction potential has been classified in terms of levels of risk of liquefaction by Iwasaki, et al. (1982), and is shown in Table 1.

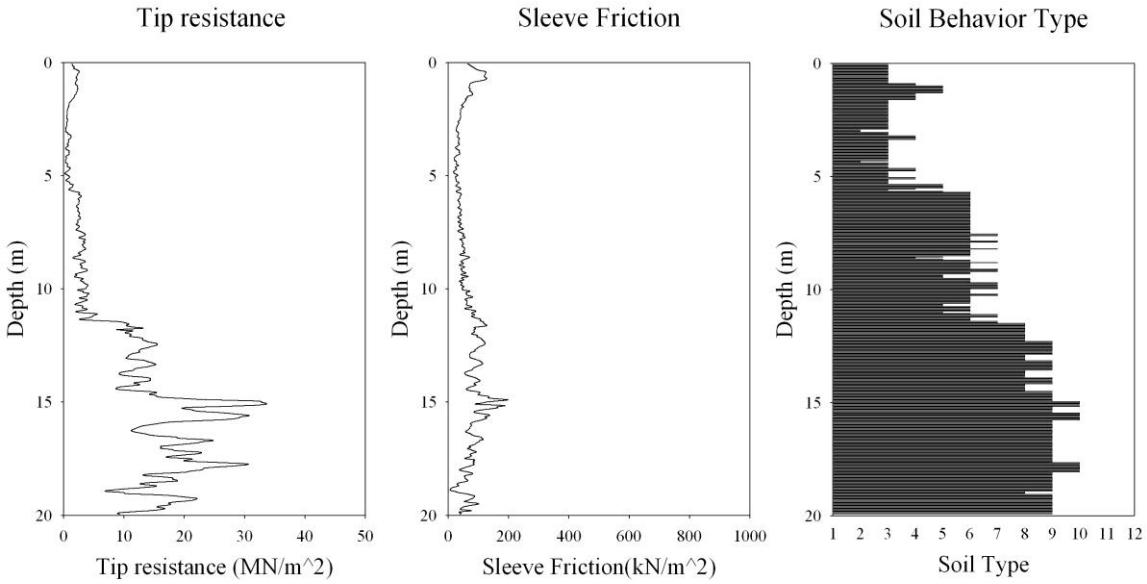

Figure 3 Example of the sequence of calculations for the factor of safety for profile VHC006, a typical profile located in the alluvial surfical unit. a) Tip resistance, b) Sleeve friction, and c) Soil type (Robertson, 1990)

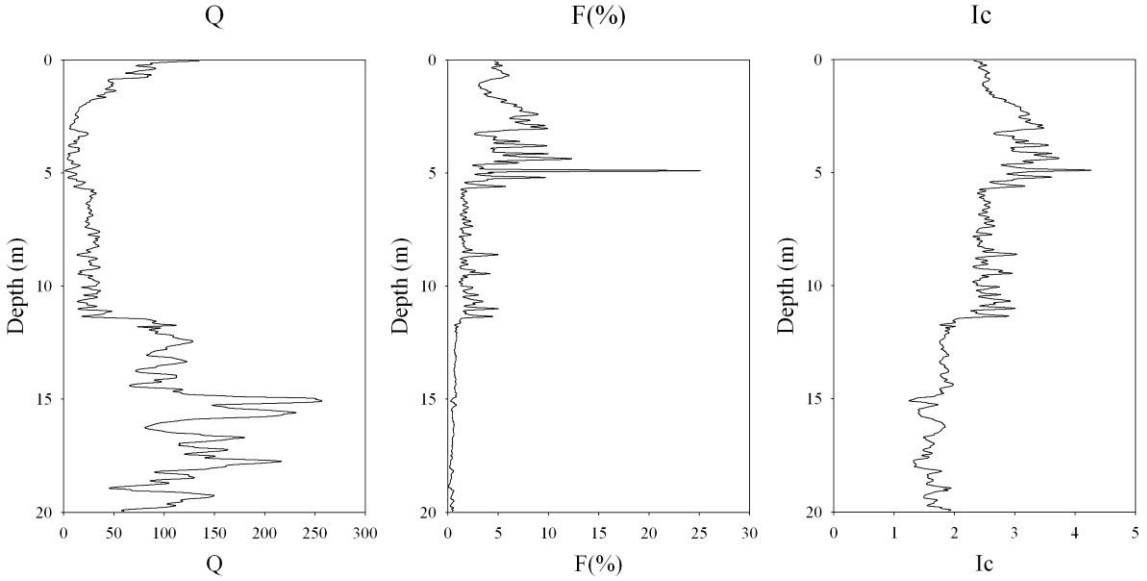

Figure 3 d) Q: normalized tip resistance, e) F: normalized sleeve friction, and f) Soil behavior type index

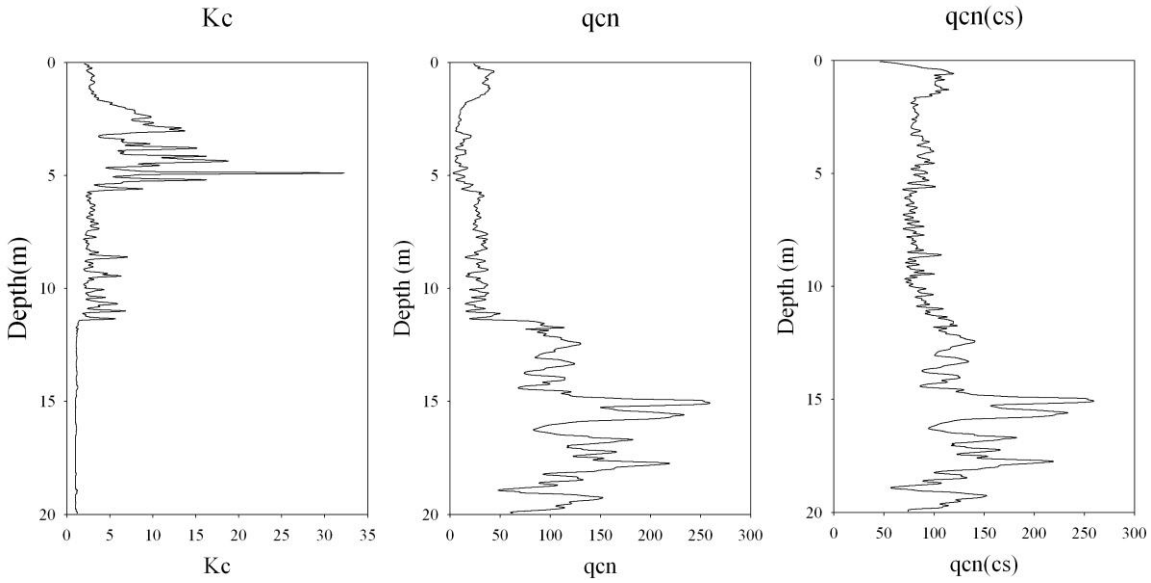

Figure 3 g) K_c: correction factor, h) q_{cn}: normalized tip resistance for overburden stress, and i) $q_{cn(cs)}$: tip resistance corrected to a clean sand

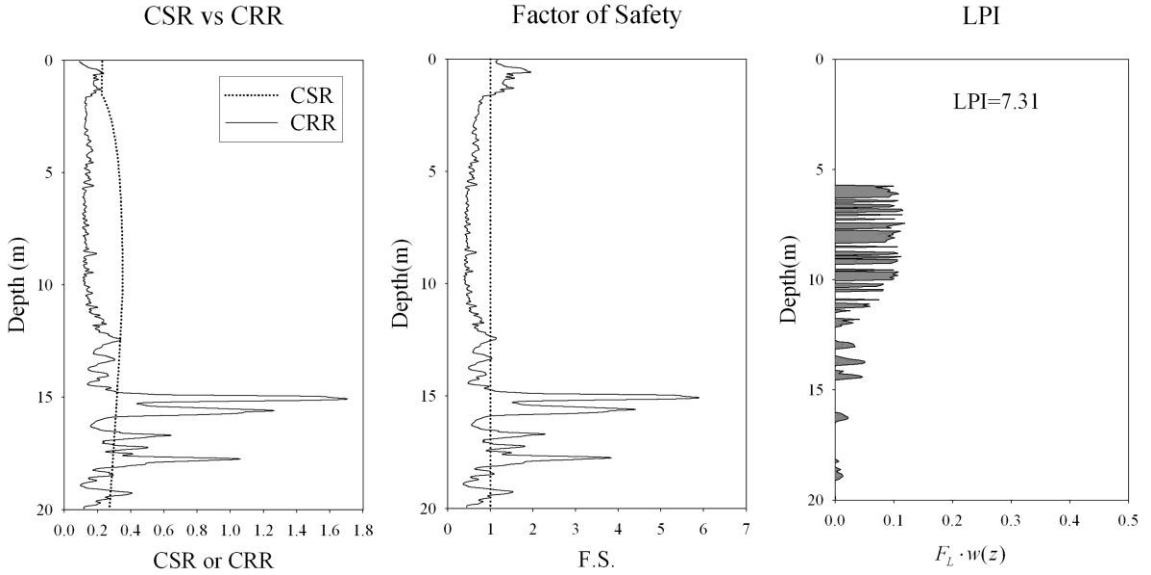

Figure 3 j) CSR and CRR, k) factor of safety, l) weighted liquefaction potential integrand $F_L \cdot w(z)$

.

Table 1 Classification of liquefaction potential (Iwasaki et al., 1982).

Liquefaction Potential Index (LPI)	Liquefaction Potential Classification
0	Non-liquefiable
$0 < LPI \leq 2$	Low
$2 < LPI \leq 5$	Moderate
$5 < LPI \leq 15$	High
$LPI > 15$	Very High

3 Liquefaction calculation for scenario earthquakes

The scenario earthquakes were chosen based on the modal earthquakes from the deaggregation of the probabilistic seismic hazard (Harmsen et al., 1999). While the probabilistic seismic hazard is a sum of the contributions from all possible source magnitudes at all source distances, the deaggregation analyzes which source contributes the most to that hazard. The significance of the events is directly related to geologic information on historic and pre-historic information that went into the PSHA calculation. The New Madrid type event was input into the seismic hazard estimation with parameters on magnitude determined based on historical felt effects (ie. Hough et al., 2000; Nuttli, 1983) and recurrence intervals based on paleoliqefaction evidence in ancient sand blows (Frankel et al., 1996; Tuttle et al., 1999; Tuttle and Schweig, 1995). The magnitude 7.7 modal earthquake reflects this information. While specific fault recurrence rates and magnitudes for historic earthquakes in the Wabash fault zone were not constrained well enough to serve as direct input to the probabilistic seismic hazard estimate, there is a history of magnitude 6.2 to 7.3 events in the Wabash fault zone over the last 10,000 years (Obermeier, 1998; Obermeier et al., 1991; Olson et al., 2005) that are comparable to the modal earthquake for PGA. Therefore we believe there is sufficient evidence to support the use of these modal earthquakes as scenario earthquakes for the liquefaction analysis.

In this study, we calculate the LPI using the procedure described in the previous section at each CPT site for the two scenario earthquakes of magnitude 6.5 and 7.7. We use peak ground accelerations ranging from 0.2 to 0.5 g for a_{max} which were derived from the 2% probability of exceedence PSHA maps (Haase et al., 2006). The results are shown in Figure 4.

We use the soil descriptions and geologic data to define the general characteristics of the map region. The nine quadrangle map area is divided into 5 sub-groups based on the engineering soil profile data: Group1: the predominant geologic unit is River Alluvium and includes recent and old Ohio river sediments (Qal, Qall, Qat1); Group 2: the predominant geologic unit is Terrace Alluvium (Qlat, Qat2); Group 3: the predominant geologic unit is Lacustrine Terrace Deposit (Qlt); Group 4: Loess (Ql); Group 5: Other minor units including man-made land. There are sufficient CPT data in the first three sub-groups, even though these data are not uniformly located, to characterize their properties statistically. No CPT data is available in the Loess surficial unit, however these areas typically have a thin layer of deposits over bedrock and are not expected to liquefy. Artificial fill and other units in the fifth group cannot be characterized based on their geologic environment, but require engineering data on their origin, and are thus beyond the scope of this study. The LPI results are listed in **Table 2** for each of the CPT data from the first three sub-groups to illustrate how the surficial geology affects the liquefaction calculations. Examples of typical soil profiles from each subgroup and the factor of safety for each element in the profiles are shown in the Appendix.

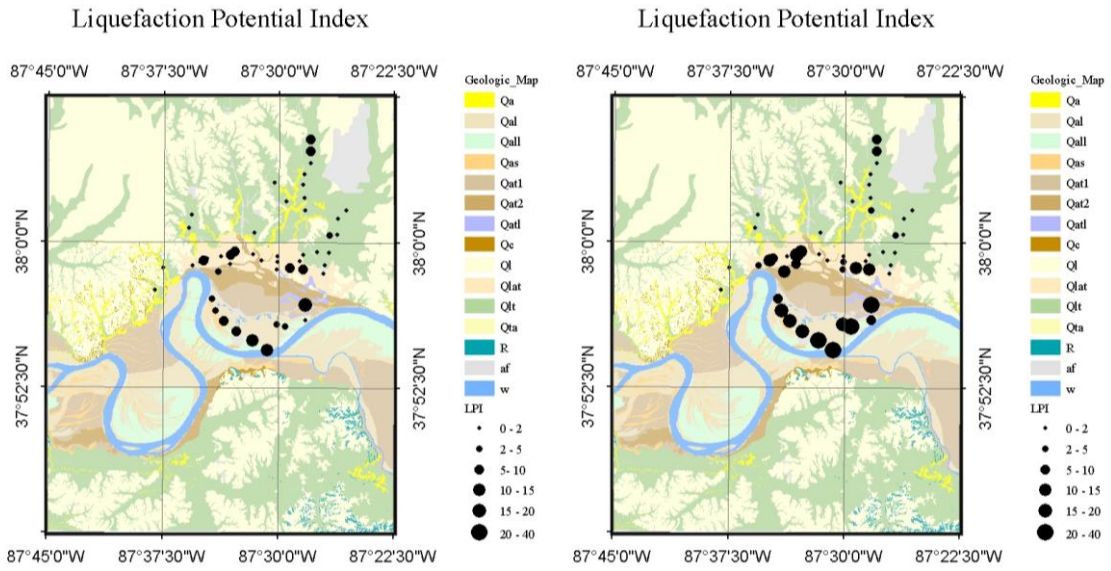

Figure 4 Calculation of liquefaction potential index from the CPT profiles for an earthquake with Mw= 6.5 (Left) and Mw= 7.7 (Right).

Table 2 LPI for each CPT measurement listed by surficial geologic unit and regrouped based on engineering geology soil characteristics.

SITE	LPI (MW=6.5)	LPI (MW=7.7)	LABEL	Geologic Description	Sub Group
VHC005	4.41	17.10	Qal	River alluvium	Group 1
VHC006	7.31	17.81	Qal	River alluvium	
VHC007	2.83	15.68	Qal	River alluvium	
VHC008	12.41	26.05	Qal	River alluvium	
VHC009	11.16	24.85	Qal	River alluvium	
VHC010	7.30	17.90	Qal	River alluvium	
VHC001	2.11	21.11	Qall	River alluvium, levee deposit	
VHC002	0.48	5.96	Qall	River alluvium, levee deposit	
VHC003	16.74	37.06	Qat1	Terrace alluvium	
VHC012	7.14	11.93	af	Artificial fill	Group 2
VHC025	0.33	6.45	Qat2	Terrace alluvium	
VHC035	3.15	10.10	Qat2	Terrace alluvium	
VHC013	0.13	0.66	Qlat	Terrace alluvium and paleolevee deposit	
VHC015	0.10	0.28	Qlat	Terrace alluvium and paleolevee deposit	
VHC016	7.73	12.36	Qlat	Terrace alluvium and paleolevee deposit	
VHC017	0.88	2.03	Qlat	Terrace alluvium and paleolevee deposit	
VHC018	0.80	3.00	Qlat	Terrace alluvium and paleolevee deposit	

VHC019	0.70	1.97	Qlat	Terrace alluvium and paleolevee deposit	
VHC020	0.47	1.11	Qlat	Terrace alluvium and paleolevee deposit	
VHC021	9.65	13.82	Qlat	Terrace alluvium and paleolevee deposit	
VHC023	0.04	0.40	Qlat	Terrace alluvium and paleolevee deposit	
VHC024	0.10	0.67	Qlat	Terrace alluvium and paleolevee deposit	
VHC026	0.39	0.64	Qlat	Terrace alluvium and paleolevee deposit	
VHC027	1.32	8.34	Qlat	Terrace alluvium and paleolevee deposit	
VHC028	0.00	0.30	Qlat	Terrace alluvium and paleolevee deposit	
VHC032	0.51	3.11	Qlat	Terrace alluvium and paleolevee deposit	
VHC033	8.14	11.76	Qlat	Terrace alluvium and paleolevee deposit	
VHC034	8.62	15.06	Qlat	Terrace alluvium and paleolevee deposit	
VHC011	0.09	0.79	Qlt	Lacustrine terrace deposit	Group 3
VHC014	0.41	2.27	Qlt	Lacustrine terrace deposit	
VHC022	0.00	0.00	Qlt	Lacustrine terrace deposit	
VHC029	0.07	0.81	Qlt	Lacustrine terrace deposit	
VHC030	0.06	0.09	Qlt	Lacustrine terrace deposit	
VHC031	0.00	0.28	Qlt	Lacustrine terrace deposit	
VHC037	0.06	0.35	Qlt	Lacustrine terrace deposit	
VHC038	0.40	1.28	Qlt	Lacustrine terrace deposit	
VHC039	0.23	1.25	Qlt	Lacustrine terrace deposit	
VHC040	0.10	0.21	Qlt	Lacustrine terrace deposit	
WKC001	0.06	0.07	Qlt	Lacustrine terrace deposit	
WKC002	2.63	4.16	Qlt	Lacustrine terrace deposit	
WKC003	0.02	0.06	Qlt	Lacustrine terrace deposit	
WKC004	0.38	0.80	Qlt	Lacustrine terrace deposit	
WKC005	0.30	0.74	Qlt	Lacustrine terrace deposit	
WKC006	5.32	7.32	Qlt	Lacustrine terrace deposit	
WKC007	0.01	0.27	Qlt	Lacustrine terrace deposit	
WKC008	0.00	0.37	Qlt	Lacustrine terrace deposit	
WKC009	5.66	9.12	Qlt	Lacustrine terrace deposit	
WKC010	0.00	0.00	Qlt	Lacustrine terrace deposit	

3.1 Results for the river alluvium region

CPT profiles in the river alluvium subregion group 1 (see Appendix Figure A1) typically have extensive sand and gravelly sand units below about 10 m, and finer silt and clay layers above that. The factor of safety for liquefaction in the river alluvium region is calculated using the method described above. The factor of safety in the deeper older Ohio river sand and gravel deposits is highly variable below 10m in most profiles, primarily because the tip resistance is quite variable (Figure 3a) and sometimes

sufficiently high to give the CRR high enough values to resist liquefaction. Those layers that do not have a sufficiently high CRR to resist liquefaction make a large contribution to the LPI. Surprisingly, some profiles with sand units near the surface, such as VHC007, do not make a large contribution to the LPI, because of very high tip resistances, probably due to over consolidation. The intermediate depth silty sand layers do make a significant contribution to the LPI. The unit near the surface was identified in many of the CPT profiles in this region as high clay and clayey silt content. When the soil behavior type index of these layers was evaluated, they typically have $I_c > 2.6$ indicating they are clay layers that are not susceptible to liquefaction (see section 3.4 below). Figure 5 shows the soil behavior type index Ic computed for all clay rich soil elements in the CPT dataset a sa function of normalized friction ratio F. Superimposed on this is the domain of susceptible liquefaction from Robertson and Wride (1998) and Youd (2001). These layers, indicated with a red 'x' for the factor of safety in Figure 3a, do not contribute to the LPI. However, the results are overall very high for LPI for all sites in the river alluvium.

3.2 Results for the lacustrine region

Profiles in the lacustrine region (see Appendix Figure A2) typically have extensive clay and silt layers in the upper 20m. The method that is used to calculate liquefaction susceptibility was originally developed for sandy soil, so there is a criterion that the soil behavior index I_c is less than 2.4 for the method to be used. Soils with behavior index greater than 2.6 are clay soils that are not susceptible to liquefaction (Robertson and Wride, 1998). This is the case for most of the profiles. The relatively homogeneous clay layers exhibit different properties in approximately the upper 7 m where tip resistances are much greater leading to greater factors of safety. The factor of safety for profiles within the lacustrine region is also shown in the Appendix. Those data with $I_c > 2.6$ are indicated with a red 'x' in the factor of safety profiles. Data with $2.4 < I_c < 2.6$, which require additional testing to determine their liquefaction susceptibility are indicated with a blue triangle. These data are examined in more detail in section 3.4. Silt and silty clay that have soil behavior type index between the range of 2.4 and 2.6 critically affect the values of liquefaction potential index that are obtained.

3.3 Results for the terrace alluvium

The soil profiles within the deposits of the terrace alluvium region are more complex as they contain highly variable sequences of silty sand, clayey sand, and sandy clay from overlapping transitional depositional environments (see Appendix Figures A3 and A4). There is little consistency of the soil profiles over the region as a whole, but there is some indication of a weak correlation with depositional history. On the west side of the region, sandy silt and silty sand that may correspond to river overbank deposits appear midway through the profiles. The depths of these units vary with distance from the current river bed and have extensive layers of clay in locations where the soil profile may be filling in older stream valleys that accumulated clay soils in the lacustrine high-stands. The furthest west profiles of the region typically have high tip resistance and resulting high factor of

safety for the intermediate depth sandy silt unit (see Appendix). Clay units found below this depth are predominantly excluded from the LPI calculation, once again because of the Ic > 2.6 criterion. Silty sand units below this intermediate depth make a large contribution to the LPI. Towards the center of the region, there are more extensive sandy silt and silty sand units that do not have high tip resistance. These have a much lower factor of safety and contribute greatly to the LPI. Further east, even though the soil type determined based on CPT and the calculated factor of safety at nearby sites have similar values through the entire depth, for example VHC017 and VHC016, the liquefaction potential index is quite different at the two sites, primarily due to small differences in the number of layers that satisfy the I_c criterion < 2.6. The furthest east profiles have most values of I_c > 2.6 and therefore result in low LPI values. Due to the high variation of the soil properties and the resulting liquefaction susceptibility, it is very difficult to extrapolate the soil profile properties to nearby sites. In order to construct a liquefaction susceptibility map for this complex region, a probabilistic method is more appropriate.

3.4 Evaluating liquefaction potential for silty and clayey soil

Generally, there are two criteria based on soil index properties that are used for the evaluation of liquefaction susceptibility of silty and clayey soils. The first method is based on soil behavior index (I_c) and the normalized friction ratio (F) from CPT data (Robertson and Wride, 1998). According to the first method, soils are not susceptible to liquefaction if the soil behavior index I_c > 2.6 and normalized friction ratio (F) > 1.0%. Soils with I_c between 2.4 and 2.6 or with I_c > 2.6 and F < 1 require further laboratory testing before their susceptibility to liquefaction can be determined. Another testing method, which is based on Atterberg limits, was developed by Bray et al., (2006) for the evaluation of liquefaction susceptibility. Depending on the plastic index (PI) and the ratio of water content (w) to liquid limit (LL), clayey soils can be determined to be susceptible to liquefaction or not.

To examine the extent of this problem in our dataset, soils containing clay-rich layers in the CPT data are plotted on an I_c-based criteria chart (Figure 5). We presume that soils with I_c < 2.4 will be vulnerable to liquefaction, so the factor of safety is computed and used for the liquefaction potential index (LPI). For soils with (I_c) > 2.6 and normalized friction ratio (F) > 1.0%, we consider that they are not susceptible to liquefaction, so the contribution to the liquefaction potential index (LPI) is set to zero at that particular depth point even though the factor of safety is less than 1. If the soils lie in the test required zone, then the assessment of liquefaction susceptibility requires more investigation. It was found that the profiles containing soil elements that fell into this category were confined mostly to a relatively localized region near profiles WKC006 and WKC009 in the northern part of the lacustrine unit (Figure 1).

Because data on the liquid limit and plasticity index were not collected for this CPT dataset, we investigated the properties of similar soils from other geotechnical studies in the same localized region, which did include Atterberg limits. These were compiled and plotted on a plasticity index-based criteria chart (Figure 6). From these tests, we see that

most of the soils in this region belong to the zone of "not susceptible" to liquefaction. Therefore, we conclude that for this case, clay-rich soils, which fall into the "test required" region, are not susceptible to liquefaction and make no contribution to the calculation of the liquefaction potential index. This assumption was retained in the final liquefaction maps.

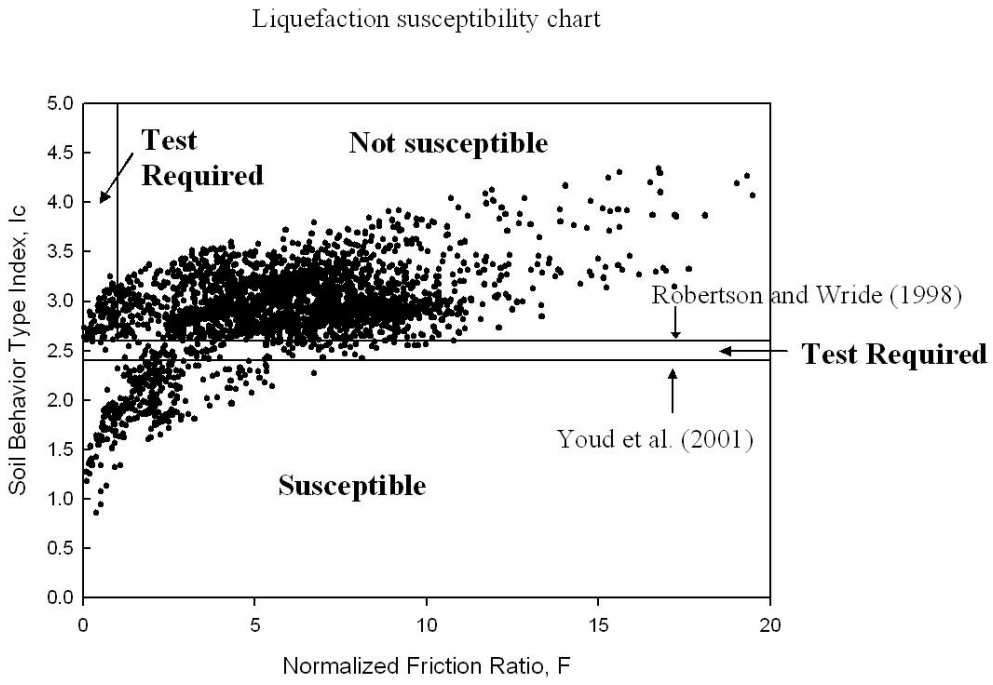

Figure 5 Soil behavior index, I_c, and friction ratio F plotted for all clay-rich soil elements in the CPT dataset.

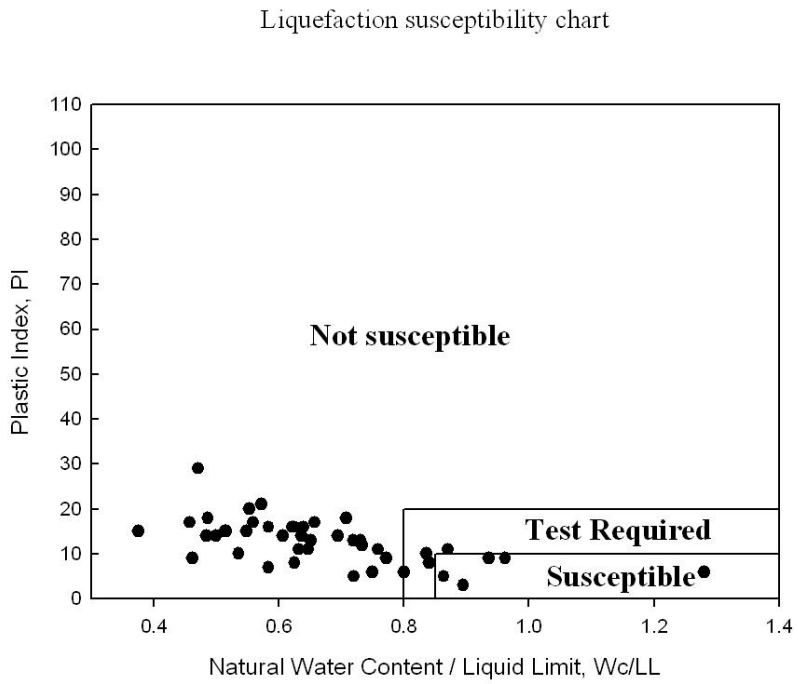

Figure 6 Test datasets of plasticity index, water content, and liquid limit from clay units near the CPT profiles within the lacustrine subregion that required further testing to determine liquefaction susceptibility.

4 Mapping liquefaction potential using a probability-based method

While we do not have a dense sampling of CPT data throughout the entire study area, we believe there is sufficient CPT data to determine the statistical properties of the soil textures found within profiles in each of the subgroup regions. Other required information for calculating the factor of safety and LPI that depend on the location are the depth of the ground water table, the thickness of the soil layer and the level of acceleration a_{max}. The approach we applied was to determine at each point in the study region the distribution of the liquefaction potential index (LPI) based on Monte Carlo sampling of the distributions of the four parameters from which LPI are calculated. For this probability-based method, the four variables of ground water level, thickness of the soil deposits, distribution of soil textures within the surficial geologic unit, and peak ground acceleration are evaluated at every 0.1 degree grid point.

The ground water table depth at each point was selected from a distribution with mean given by the depth at that point shown in Figure 2 and a standard deviation of 7.2 m. The same method was used to select the soil deposit thickness. It was based on the bedrock surface determined from logs and refraction profiles in a previous study, as it was also required for the probabilistic hazard analysis (Haase et al., 2006). Data from the Indiana

Department of Natural Resources, 900 Indiana Geological Survey water well logs, 230 seismic P-wave refraction profiles, and bedrock elevation points from Kentucky Geologic Survey oil, gas, and water well logs were integrated to determine the thickness of soil deposits and depth to bedrock. Contours of the thickness of soil deposits were calculated using local polynomial interpolation and the errors were evaluated to be on the order of +/- 6 m (Figure 7a). At each point, the thickness was selected from a distribution with this mean thickness and standard deviation.

The probabilistic seismic hazard map for the nine quadrangle region surrounding Evansville takes into account amplification due to the near-surface geologic structure. The value of peak ground acceleration with 2% probability of being exceeded in 50 years from the probabilistic seismic hazard map is used as the a_{max} variable for the liquefaction evaluation. While this is not strictly the PGA associated directly with the scenario earthquake of magnitude 6.5 or magnitude 7.7, it does correspond to the modal earthquake, which is comparable in size to these scenario earthquakes. The PGA values vary moderately in space (Figure 7). The PGA value was slected at a specific grid point and used for a_{max} in all of the the Monte Carlo simulations for LPI at that grid point.

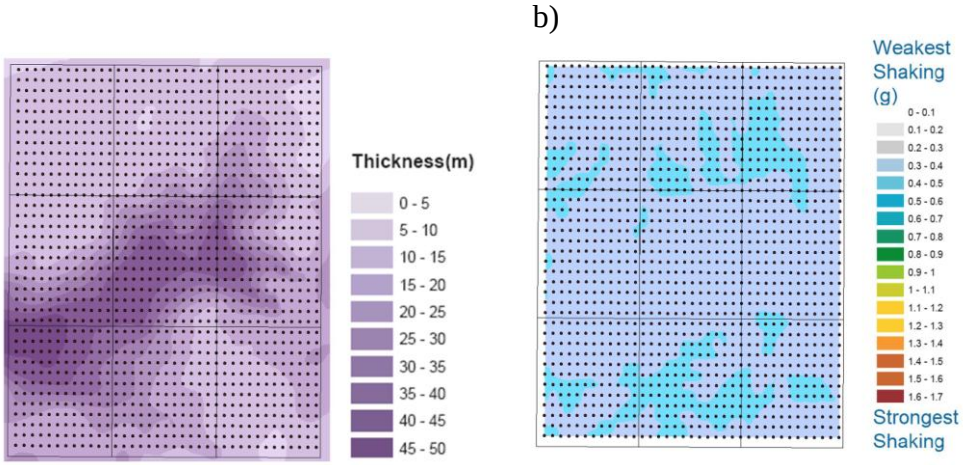

Figure 7 Location specific parameters for calculating the liquefaction potential index were selected from maps for a) thickness of the soil above bedrock b) the level of peak ground acceleration with 2% probability of being exceeded in 50 years.

The CPT data were split into 3 subregion groups based on surficial geology and general characteristics of the CPT soil description. The three subgroups are the following: Group 1: Qal, Qall, Qat1; Group 2: Qlat, Qat2; Group 3: Qlt. Then the distributions of tip resistance and sleeve friction in the CPT profile were evaluated for each group. The lognormal mean and standard deviation of tip resistance and sleeve friction at every 2 meter depth were calculated. Examples are shown in Figure 8 of the variation of properties with depth, and in Figure 9 an example is shown of the variation of the properties at one depth interval. Based on these statistics, 1000 random values of tip resistance and sleeve friction at each 2 meter depth point are generated for each grid point, depending on which subgroup it falls into.

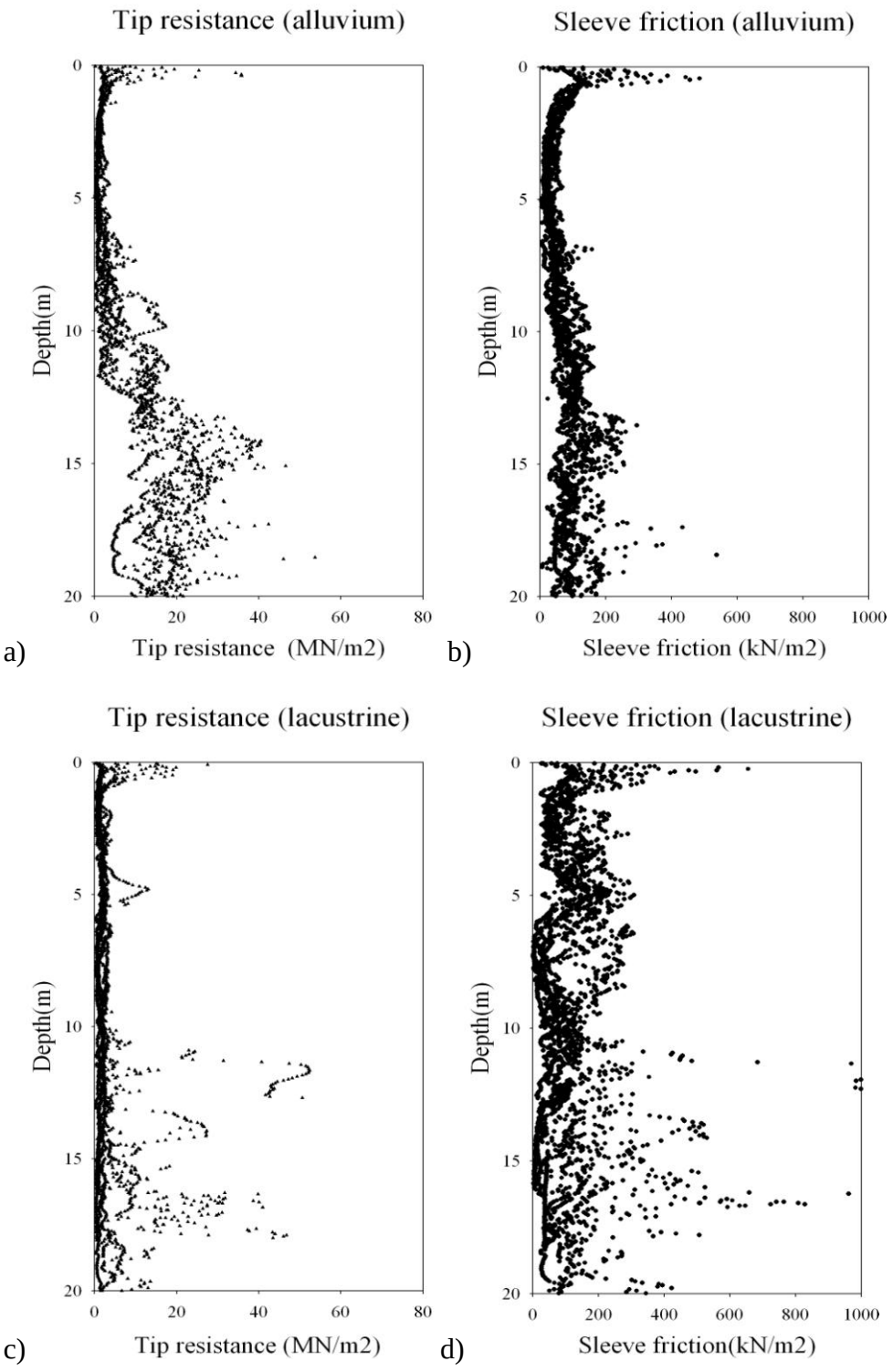

Figure 8 a) Examples of the variation with depth for all profiles in the subregion group 1 (river alluvium) of a) the tip resistance q_c and b) sleeve friction F_s. Examples of the variation with depth for all profiles in the subregion group 3 (lacustrine) c) of tip resistance q_c and d) sleeve friction F_s .

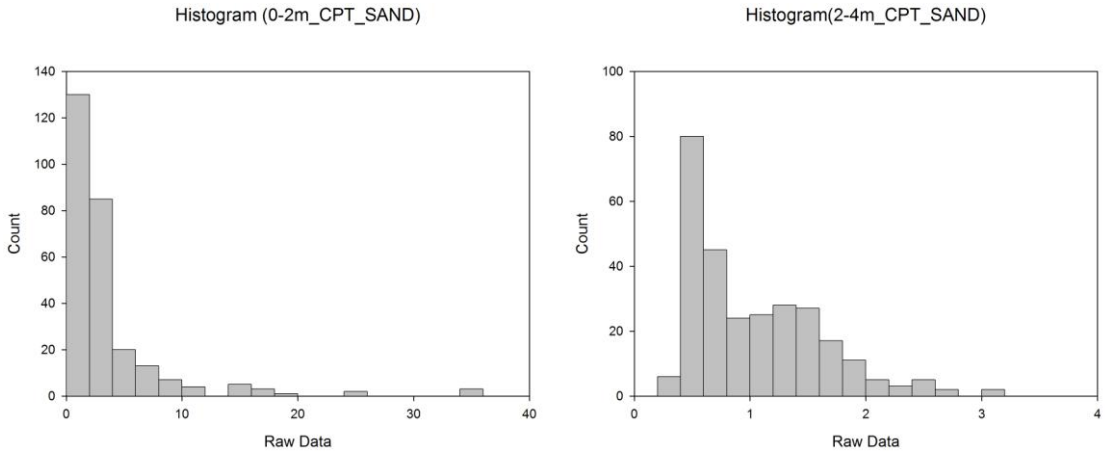

Figure 9 Examples of the distributions of tip resistance for the layer at 0-2m depth (left) and 2-4m depth (right) for CPT profiles in subgroup 1.

For each of the random profiles of tip resistance and sleeve friction, values for total soil thickness and water table were sampled from their respective distributions. With the value of amax appropriate for that location, 1000 realizations of the LPI at each grid point were calculated. The calculation was done individually for the two scenario earthquakes of magnitude 6.5 and 7.7 with peak ground accelerations ranging from 0.2 to 0.5 g. The value of a_{max} is used in the calculation of CRR, and the magnitude scaling factor is based on the scenario earthquake magnitude. The cumulative frequency distributions of LPI are calculated for each subgroup for the CPT data and for the synthetic LPI. For subgroup 1, primarily river alluvium, the percent of LPI values that exceeds 5 is 69.9%. For subgroup 2, primarily terrace alluvium, the percent of LPI values that exceeds 5 is 34.9%. For subgroup 3, primarily lacustrine, the percent of LPI values that exceeds 5 is 1.9%. The spatial distribution of the mean LPI is shown in Figure 10.

From the cumulative frequency distribution of LPI at each grid point, the probability of exceeding LPI of a specific value (5 or 15) for constant magnitude of earthquake (Mw) is then calculated. Within the lacustrine group, most of the region has low LPI; the probability that LPI >5 is only 20~30 %. Within the river alluvium group, most of the region has high LPI; the probability that LPI >5 is 80~100 %. Within the transition group, the soil sequences are highly variable, the probability that LPI >5 can vary greatly. These results are shown in Figure 11 and Figure 12. Much of the Evansville urban area is built on soils where the probability that LPI >5 is more than 60 % for a M7.7 New Madrid type event.

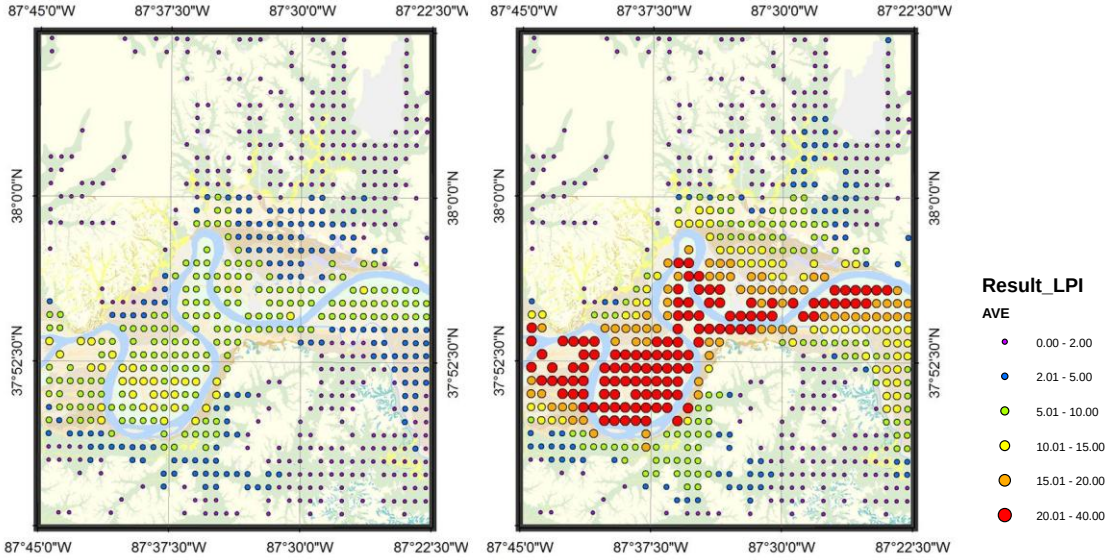

Figure 10 Mean LPI for (left) magnitude 6.5 scenario earthquake and (right) magnitude 7.7 scenario earthquake.

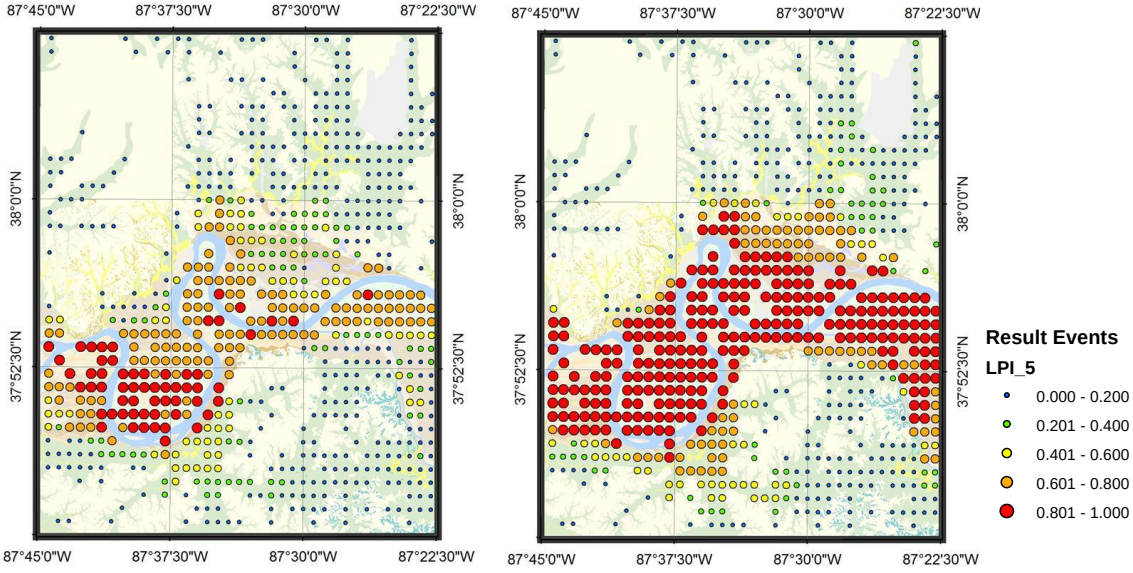

Figure 11 Probability that LPI > 5 for (left) magnitude 6.5 scenario earthquake and (right) magnitude 7.7 scenario earthquake.

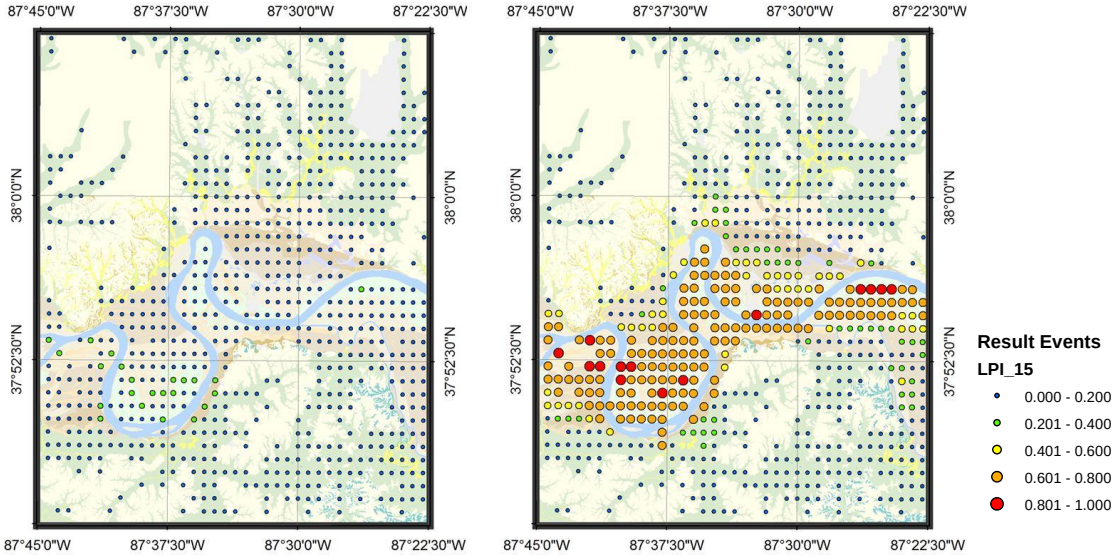

Figure 12 Probability that LPI > 15 for (left) magnitude 6.5 scenario earthquake and (right) magnitude 7.7 scenario earthquake.

5 Discussion

In order to provide a basis for discussion of our results relative to previous results in the region that were determined using SPT data, we compared LPI results from individual profiles determined from CPT and SPT where both types of data were available from the same sites. For the SPT data, we used the method of Youd et al. (2001) to estimate liquefaction potential index. For each site, there were several SPT logs available.

Table 3 Comparison of LPI calculated using SPT and CPT data for several sites in close vicinity within the lacustrine subregion group 3.

SPT site	LPI	CPT site	LPI
I-164 bridge	14.10	WKC007	0.05
I-164 site 1	0.0 0.0 0.0 0.0 0.0 0.0	VHC030	0.06
I-164 site 2	0.0 0.12 0.0	VHC029	0.19

	0.0 0.0		
I-164 site 3	0.0 0.0 0.0	VHC014	0.85

Table 4 Comparison of LPI calculated using SPT and CPT data for several sites in close vicinity within the river alluvium subregion 1.

SPT site	LPI	CPT site	LPI
I-164 site 4	34.46 31.12 27.79 29.89 21.03 32.53	VHC003	37.06

In this comparison there was originally a large difference between the LPI calculated based on CPT and SPT data. We found that the high values for LPI from the SPT calculation were due to layers with soil classifications 1-6. Given that these layers would likely be too clay or silt-rich to liquefy (similar philosophy to applying a criterion on I_c), we excluded these values from the calculation. After that adjustment, the LPI's calculated from the SPT agreed acceptably with the CPT (Table 3 and Table 4). Having shown that the CPT and SPT data are comparable, we discuss our results in the context of previous studies.

Bobet et al. (2001) performed a soil response analysis at several SPT locations within the Wabash Valley in southwestern Indiana using the equivalent linear one-dimensional wave propagation analysis method (SHAKE program, Idriss and Sun, 1992). Using the profile of peak acceleration with depth obtained from the soil response analysis, the actual cyclic stress ratio and the critical cyclic stress ratio required to initiate liquefaction are compared to evaluate the liquefaction potential. Two sites from that study are within the map region for our project and one showed likelihood for liquefaction. This agreed with our results in that area.

Kayabali (1993) produced a map showing the vulnerability of Evansville soils to liquefaction using SPT and the stress reduction factor determined from CPT data. He used sampled data primarily from within the our terrace alluvium subregion 2, and found that the area at highest liquefaction potential very close to the Ohio river, but very high variation of liquefaction potential even within his smaller map region, which is consistent with our results. Eggert (1994) suggested that a more comprehensive evaluation of the liquefaction hazard in the Evansville area should be carried out. Our study complements this earlier study by extending it to a larger study area.

6 Conclusions

The objective of this study was to provide a comprehensive map for liquefaction hazard in and around Evansville. The study used scenario earthquakes of magnitude 6.5 and 7.7 decided in collaboration with the Tri-state Earthquake Advisory Group (USGS, 2004). For the liquefaction study, cone penetrometer test (CPT) data were collected (Holzer, 2003) that sample the principal surficial geologic units (Moore, et al., 2007). The factor of safety against liquefaction for each CPT location was calculated using a standard method (Robertson and Wride, 1998) based on the cyclic resistance ratio and cyclic stress ratio and the properties of the soil column. These show high variability of LPI for those samples in the terrace alluvium subregion, high LPI values in the river alluvium subregion and low LPI in the lacustrine subregion. We established the probability distributions for liquefaction potential for each region using the properties of individual soil layers from the same CPT data set and created maps of the probability of exceeding a given liquefaction potential index. The resulting maps quantify the distribution of high liquefaction potential sites in the river alluvium where the soil profile contains more sand, and describe the contrasting region of lacustrine deposits that predominantly include clayey soil with lower liquefaction susceptibility. From the cumulative frequency distribution of LPI at each grid point, the probability of exceeding LPI of a specific value (5 or 15) for constant magnitude of earthquake (Mw) is then calculated. Within the lacustrine group, most of the region has low LPI, where the probability that LPI >5 is only 20~30 %. Within the river alluvium group, most of the region has high LPI, where the probability that LPI >5 is 80~100 %. Within the transition group, the soil sequences are highly variable, so using a probabilistic approach is critical. The probability that LPI >5 can vary greatly. Much of the Evansville urban area is built on soils where the probability that LPI >5 is more than 60 % for a M7.7 New Madrid type event.

7 Acknowledgements

This work was supported by USGS National Earthquake Hazards Reduction Program grant (07HQGR0058). We thank Tom Holzer and the liquefaction hazard group at the USGS for making available the CPT data. We thank Ron Counts at the KGS for providing water well and boring data. We thank Antonio Bobet for assistance with the liquefaction analysis method.

8 Appendixes

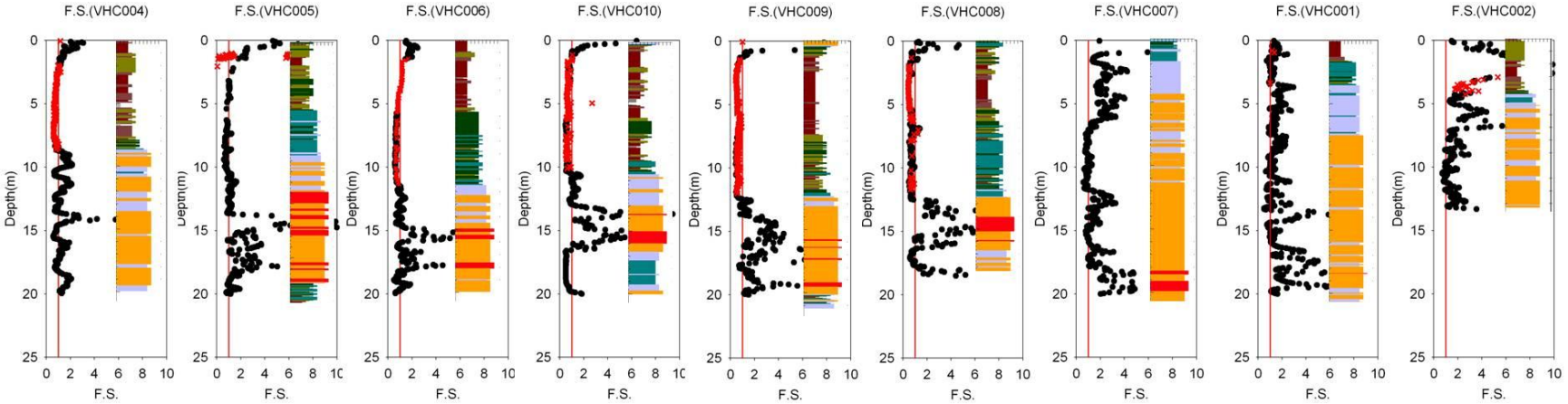

Figure A1 Subgroup-1 river alluvium profiles and calculated factor of safety with soil units taken from Holzer (2003). Units with soil behavior index I_c less than 2.6 do not contribute to the LPI and are indicated with the factor of safety in red.

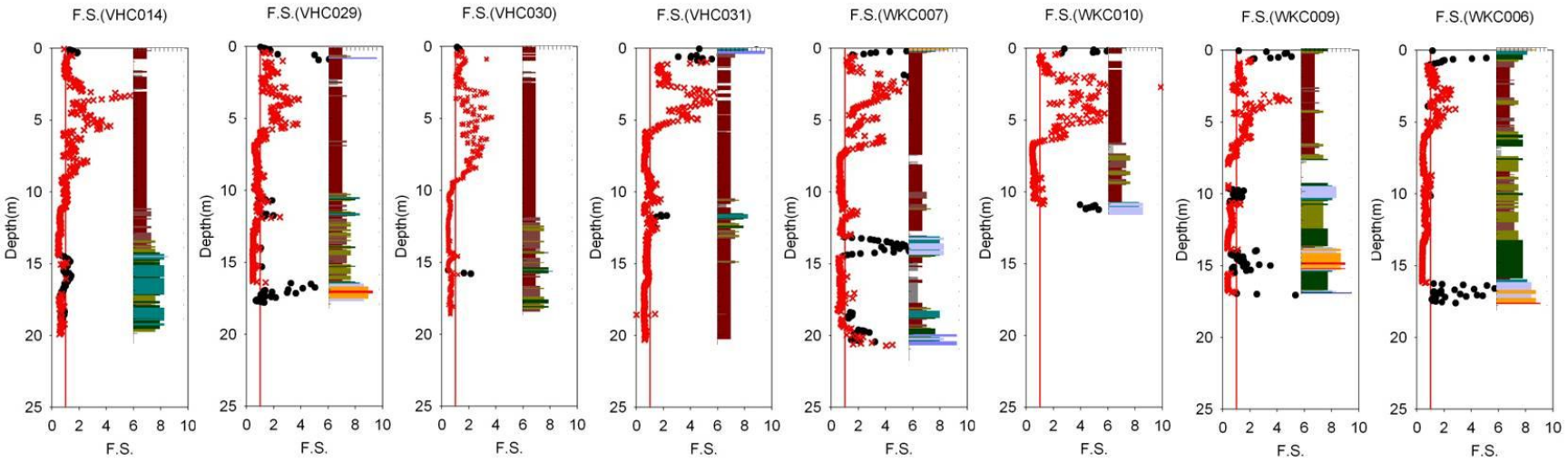

Figure A2 Subgroup-2 lacustrine profiles and calculated factor of safety with soil units taken from Holzer (2003). Units with soil behavior index I_c less than 2.6 do not contribute to the LPI and are indicated with the factor of safety in red.

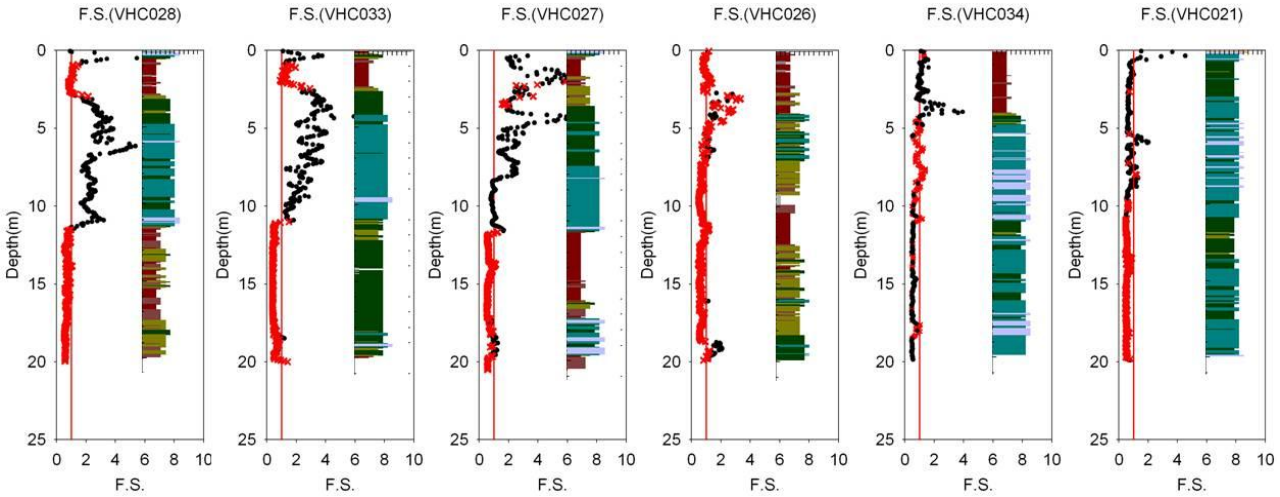

Figure A3 Subgroup-3 western terrace alluvium profiles and factor of safety with soil units taken from Holzer (2003). Units with soil behavior index Ic less than 2.6 do not contribute to the LPI and are indicated with the factor of safety in red.

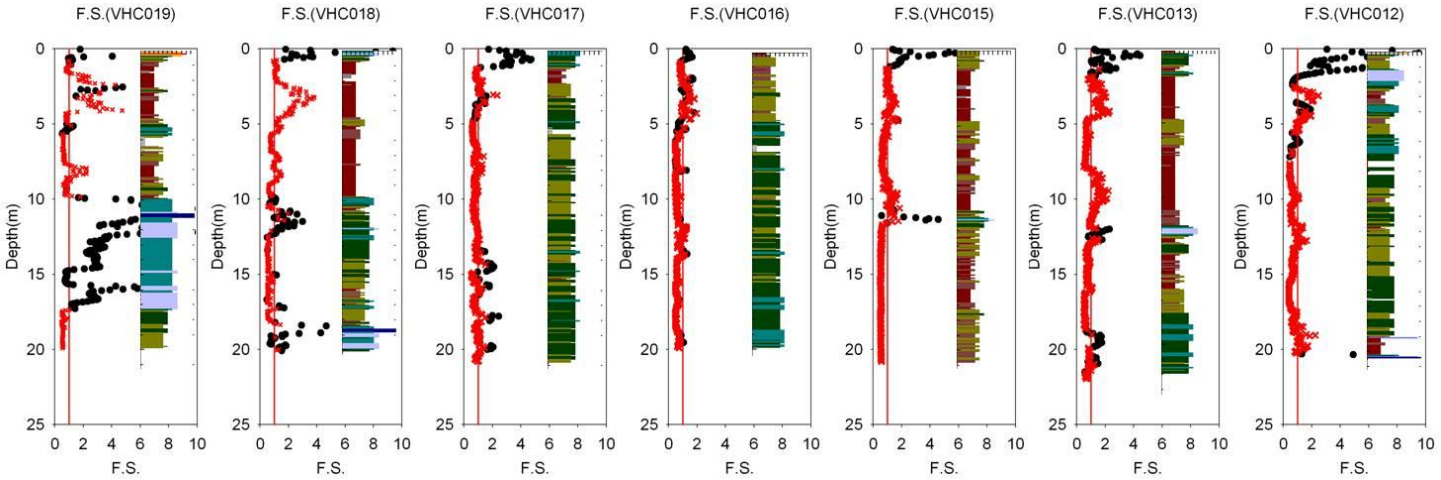

Figure A4 Subgroup-3 eastern terrace alluvium profiles and calculated factor of safety with soil units taken from Holzer (2003). Units with soil behavior index Ic less than 2.6 do not contribute to the LPI and are indicated with the factor of safety in red.

Legend for figures A1-A4.

9 References

Bobet, A., Salgado, R. and Loukidis, D., 2001. Seismic design of deep foundations, JTRP Report FHWA/IN/JTRP-2000/22. FHWA/IN/JTRP-2000/22

Project No. C-36-36GG

File No. 6-14-33, Joint Transportation Research Program, Purdue University, West Lafayette, IN.

Bray, J.D. and Sancio, R.B., 2006. Assessment of the Liquefaction Susceptibility of Fine-Grained Soils. J. Geotech. and Geoenvironmental Eng., 1332(9): 1165-1177.

Eggert, D.L., Woodfield, M.C., Bleuer, N.K. and Hartke, E.J., 1996. Geologic Terrain Map of the Indiana Portion of the Newburgh Quadrangle, Indiana-Kentucky. Open-File Studies, OFS96-09, Indiana Geological Survey, Bloomington, IN.

Eggert, D.L., Woodfield, M.C., Bleuer, N.K. and Hartke, E.J., 1997a. Geologic Terrain Map of the Daylight Quadrangle. Open-File Studies, OFS97-17, Indiana Geological Survey, Bloomington, IN.

Eggert, D.L., Woodfield, M.C., Bleuer, N.K. and Hartke, E.J., 1997b. Geologic Terrain Map of the Evansville Region, Indiana. Open-File Studies, OFS97-16, Indiana Geological Survey, Bloomington, IN.

Frankel, A. et al., 1996. National seismic hazard maps: documentation June 1996, U.S. Geological Survey Open-file Report 96-532, USGS.

Gray, H.H., 1989. Quaternary Geologic Map of Indiana, Indiana Geological Survey Miscellaneous Map 49, 1:500,000. Indiana Geological Survey, Bloomington, IN.

Haase, J.S., Nowack, R.L. and Choi, Y.S., 2006. Probabilistic seismic hazard assessment including site effects for Evansville, Indiana, and the surrounding region. 05HQGR0033, Purdue University, West Lafayette, IN.

Harmsen, S., Perkins, D. and Frankel, A., 1999. Deaggregation of probabilistic ground motions in the central and eastern United States. Bulletin of the Seismological Society of America, 89(1): 1-13.

Holzer, T.L., 2003. Earthquake Hazards: USGS CPT Data: Evansville, IN, Area. USGS.

Holzer, T.L., Bennett, M.J., Noce, T.E., Padovani, A.C. and Tinsley, J.C.I., 2006. Liquefaction hazard mapping with LPI in the greater Oakland, California, area. Earthquake Spectra, 22(3): in press.

Hough, S.E., Armbruster, J.G., Seeber, L. and Hough, J.F., 2000. On the Modified Mercalli intensities and magnitudes of the 1811-1812 New Madrid earthquakes. Journal of Geophysical Research-Solid Earth, 105(B10): 23839-23864.

Idriss, I.M. and Sun, J.I., 1992. User's manual for SHAKE91, Center for Geotechnical Modeling, Dept. of Civil and Environmental Engineering, University of California, Davis, CA.

Iwasaki, T. et al., 1982. Microzonation for soil liquefaction potential using simplified methods, 3rd International Conference on Microzonation, San Francisco, CA, pp. 1319-1330.

Kayabali, K., 1993. Earthquake hazard in Evansville. Ph.D. Thesis, Purdue University, West Lafayette, IN.

Lenz, J.A. and Baise, L.G., 2007. Spatial variability of liquefaction potential in regional mapping using CPT and SPT data. Soil Dynamics and Earthquake Engineering, 27(7): 690-702.

Moore, D.W. et al., 2007. Surficial geologic map of the West Franklin quadrangle, Vanderburgh and Posey Counties, Indiana, and Henderson County, Kentucky: U.S. Geological Survey Scientific Investigations Map 2967, scale 1:24,000, Menlo Park.

Munson, P.J., Munson, C.A. and Pond, E.C., 1995. Paleoliquefaction Evidence for a Strong Holocene Earthquake in South-Central Indiana. Geology, 23(4): 325-328.

Nuttli, O.W., 1983. Catalog of Central United States Earthquakes Since 1800 of mb = 3.0, St. Louis University, St. Louis. Mo.

Obermeier, S.F., 1996. Use of liquefaction-induced features for paleoseismic analysis - An overview of how seismic liquefaction features can be distinguished from other features and how their regional distribution and properties of source sediment can be used to infer the location and strength of Holocene paleo-earthquakes. Engineering Geology, 44(1-4): 1-76.

Obermeier, S.F., 1998. Liquefaction evidence for strong earthquakes of Holocene and latest Pleistocene ages in the states of Indiana and Illinois, USA. Engineering Geology, 50: 227-254.

Obermeier, S.F. et al., 1991. Evidence of Strong Earthquake Shaking in the Lower Wabash Valley from Prehistoric Liquefaction Features. Science, 251(4997): 1061-1063.

Olson, S.M., Green, R.A. and Obermeier, S.F., 2005. Revised magnitude-bound relation for the Wabash Valley seismic zone of the central United States. Seismological Research Letters, 76(6): 756-771.

Rix, G.J. and Romero-Hudock, S., 2003. Liquefaction susceptibility mapping in Memphis/Shelby County, TN. 01hqag0019, USGS, Menlo Park, CA.

Robertson, P.K., 1990. SOIL CLASSIFICATION USING THE CONE PENETRATION TEST. Canadian Geotechnical Journal, 27(1): 151-158.

Robertson, P.K. and Wride, C.E., 1998. Evaluating cyclic liquefaction potential using the cone penetration test. Canadian Geotechnical Journal, 35(3): 442-459.

Tuttle, M.P., Collier, J., Wolf, L.W. and Lafferty, R.H., 1999. New evidence for a large earthquake in the New Madrid seismic zone between AD 1400 and 1670. Geology, 27(9): 771-774.

Tuttle, M.P. and Schweig, E.S., 1995. Archaeological and Pedological Evidence for Large Prehistoric Earthquakes in the New-Madrid Seismic Zone, Central United-States. Geology, 23(3): 253-256.

Youd, T. et al., 2001. Liquefaction resistance of soils: summary report form the 1996 NCEER and 1998 MCEER/NSF workshops on evaluation of liquefaction resistance of soils. Journal of Geotechnical and Geoenvironmental Engineering, 127(10): 817-833.

Youd, T.L. and Noble, S.K., 1997. Liquefaction criteria based on probabilistic analyses.